Chemical Engineering Science 66 (2011) 2920–2934

Contents lists available at ScienceDirect

Chemical Engineering Science

journal homepage: www.elsevier.com/locate/ces

Thermodynamic optimisation of distillation columns

Filipe Soares Pinto [1], Roger Zemp [2], Megan Jobson, Robin Smith *

Centre for Process Integration, School of Chemical Engineering and Analytical Science, University of Manchester, Manchester M13 9PL, UK

ARTICLE INFO

Article history:
Received 23 June 2010
Received in revised form
27 January 2011
Accepted 14 March 2011
Available online 21 March 2011

Keywords:
Distillation
Energy
Heat transfer
Optimisation
Side reboiler
Side condenser

ABSTRACT

In this paper a methodology for thermodynamic analysis and distillation column 'targeting' is presented, with emphasis on the use of side condensers and side reboilers. Research in the past has been towards the establishment of a heat distribution curve, showing the way in which heat can be added or extracted across the different column sections. One major disadvantage of these profiles is that they refer to reversible columns, and cannot be used effectively to target for modifications in a real column.

The main feature of the proposed methodology is the introduction of a minimum driving force, defined in terms of exergy loss distribution of the existing column, to set realisable targets for side reboiling/condensing in real columns, resulting in considerable energy savings. In addition to providing realisable targets, the new approach also provides the design engineer with information about the best location to place a side exchanger, and the required additional column modifications. The methodology can be applied using conventional column models in commercial process simulation programs, but can be significantly simplified by using reboiled and refluxed absorber models in a bespoke program. Simulation results for modified designs set by the new approach, for binary and multicomponent separations, verify the feasibility of the targets. This contrasts with previous approaches, which result in temperature shifts and heat load penalties after placing side reboilers/condensers, thus requiring additional simulation time and experienced judgement.

1. Introduction

The modification and optimisation of distillation columns for better energy efficiency is a very complex task. The large number of possibilities for column configuration, including the number of stages (and reflux ratio), the location of feed stages and the use of side reboilers and side condensers renders the design a combinatorial problem. The optimisation through systematic simulation of all possible configurations is prohibitive both in time and computational effort.

A common procedure to improve the energy efficiency of distillation columns involves the use of the so-called minimum thermodynamic condition of columns, based on the use of a reversible column model. The large number of publications dealing with the calculation and application of reversible columns for a binary systems show the importance given to these profiles (Benedict, 1947; Flower and Jackson, 1964; Fonyo, 1974a, 1974b; Kayihan, 1980; Naka et al., 1980; Ho and Keller, 1987; Terranova and Westerberg, 1989).

The minimum thermodynamic condition column configuration is illustrated in Fig. 1 for a binary system. The condition of zero driving force at each stage will require a column with infinite stages and infinitely many side exchangers. For such a column, the operating line coincides with the equilibrium line along the whole column. The reversible column profile can therefore be obtained by the simultaneous solution of both the equilibrium and operating line equations.

For multicomponent systems, a reversible column condition can only be obtained for a limited sharpness of the separation. This conclusion has been reported by Fonyo (1974a, 1974b), Franklin and Wilkinson (1982) and Kaibel et al. (1989), among others. This is due to the unavoidable mixing losses that occur at the feed stage for multicomponent sharp-split distillation columns. In a multicomponent reversible column, only the lightest component can be completely removed from the bottom product, while only the heaviest is removed from the top product. Moreover, distillate and bottom compositions must be located on the line of preferred separation; i.e., a line defined from the feed and its vapour in equilibrium (Stichlmair and Herguijuela, 1992).

* Corresponding author.
E-mail addresses: zemp@feq.unicamp.br (R. Zemp), robin.smith@manchester.ac.uk (R. Smith).
[1] Current address: Aspen Technology, 195 Empire Tower, South Station Road, Yannawa, Sathorn, Bangkok 10120, Thailand.
[2] Current address: School of Chemical Engineering, University of Campinas, Av. Albert Einstein, 500, 13083-852 Campinas SP, Brazil. Tel.: +55 19 3521 3949; fax: +55 19 3521 3910.

0009-2509/$ - see front matter © 2011 Elsevier Ltd. All rights reserved.
doi:10.1016/j.ces.2011.03.022

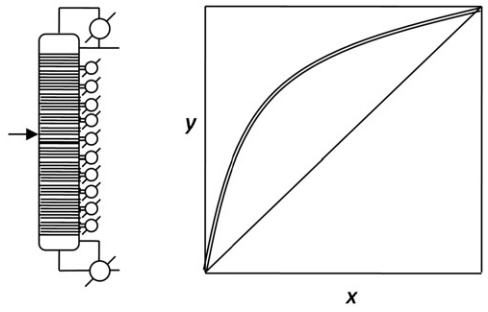

Fig. 1. Reversible column profile for a binary system.

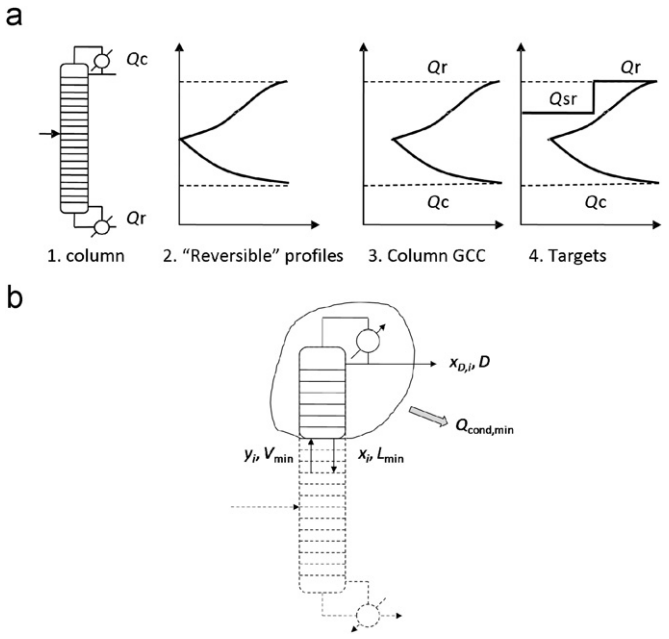

Fig. 2. Steps required to generate column targets.

For most practical multicomponent separation tasks it is therefore impossible to devise a reversible separation scheme based on a single distillation column. A procedure to obtain rigorous as-reversible-as-possible column configurations for multicomponent sharp-split separations has been developed by Koehler et al. (1991) for estimating minimum reflux conditions, but this requires extensive calculation of reversible column sections and determination of column pinch points. Along the same line, Bausa et al. (1998) proposed the rectification body method to calculate the minimum energy demand of distillation columns. More recently Danilov et al. (2007) and Petlyuk et al. (2008) proposed a general algorithm to calculate minimum reflux ratios for simple distillation columns and the construction of reversible distillation trajectories.

1.1. Temperature–enthalpy profiles

It has been proposed that reversible column profiles can be used to estimate the loads of side condensers and side reboilers of real columns, known as 'targeting', for columns operating above minimum reflux conditions (Dhole and Linnhoff, 1993; Manley et al., 1992; Bandyopadhyay et al., 1998; Demirel, 2006).

The use of reversible column profiles to target the side exchanger heat load for actual columns is shown in Fig. 2a. Mass and energy balances for reversible column sections are used to compute the reversible heat load profile. This profile is then shifted to the right on the temperature–enthalpy diagram by adding the actual heat loads of the main condenser and reboiler. Targets for intermediate heating and cooling can then be read directly from the curve. By analogy with pinch analysis, this diagram is often known as the column grand composite curve (Dhole and Linnhoff, 1993).

For binary systems the calculation of the reversible profile is a straightforward task, either computing equilibrium data or using results from converged column simulations. The procedure involves the solution of mass and energy balances for an 'envelope' over a column section from a chosen stage to the top of the column (Fig. 2b). To meet reversible conditions at the column stage the liquid leaving the stage and the vapour entering the stage are considered to be at equilibrium, $y_i^* = K_i\, x_i$. The minimum liquid and vapour traffic are then computed by solving the mass balance across the envelope, for both components:

$$V_{\min} y_1^* - L_{\min} x_1 = D x_{D,1} \tag{1}$$

$$V_{\min} y_2^* - L_{\min} x_2 = D x_{D,2} \tag{2}$$

The enthalpy deficit of the reversible column section is then computed from

$$H_{\text{def}} = H_{\text{liq,min}} - H_{\text{vap,min}} + H_D \tag{3}$$

A similar approach is used for the bottom section of the column, and together they form the reversible temperature–enthalpy profile.

The extension of this procedure to multicomponent systems is more difficult due to differences in the composition profiles between the actual and reversible column. Furthermore, the as-reversible-as-possible column has an adiabatic irreversible section, and its identification is not straightforward (Koehler et al., 1991). Aguirre et al. (1997) used the near-reversible profiles obtained by Koehler et al. (1991) to optimise the location of side exchanger subject to both thermodynamic and economic objectives, for columns operating under minimum reflux conditions.

To overcome the complexity of calculations required for multicomponent columns under actual process conditions, Dhole and Linnhoff (1993) proposed a methodology based on pseudo-binary splits between the light key and heavy key components. In this approach the key-component data from a multicomponent sharp-split distillation simulation are used in Eqs. (1) and (2) to calculate the profile as for a binary system. The main advantage of this procedure is that the results from a converged column simulation, i.e. the equilibrium composition and temperature profiles, can be used to compute the multicomponent near-reversible column profile.

However, the shape and the targets depend on the definition of the key components, and two very significant assumptions are made when using converged column simulations to obtain the profiles:

- The minimum vapour and liquid flows at a reversible stage are a function of the key component equilibrium compositions only.
- The specific enthalpies (per mole) of the liquid and vapour streams under reversible conditions are the same as under actual column conditions, although the compositions might not be the same.

A similar approach was used by Bandyopadhyay et al. (1998), who however improved the profile procedure by introducing a correction for the difference of composition between feed stream and feed stage in the actual column.

The major problem of using reversible column profiles for the identification of scope for side reboiling and side condensing is

that an ideal column (with no driving forces) is used to describe an actual column (with finite driving forces). However, only a column with an infinite number of stages can operate along reversible column sections. Furthermore, the distribution of components among the product streams in the actual column differs from the distribution in the reversible (and therefore minimum reflux) column (Seader and Henley, 2006).

For actual columns there are numerous configuration options for each specified separation, namely the number of stages and feed stage location. Each column configuration has a different heat load, and more importantly, a different distribution of driving forces inside the column.

The change of distribution of driving forces inside a column can be illustrated using the vapour–liquid composition diagram for a binary separation (Fig. 3). The distance between the equilibrium and the operating lines can be considered as the driving force for separation. Column *a* operates with 19 stages. The placement of a side reboiler at stage 14 (Column *b*) reduces the distance between the lines near the side reboiler location (a reduction of the driving force). As the number of stages is fixed, this is compensated for by a decrease in the overall driving forces along the column (the distance between the operating and equilibrium lines is increased), leading to an increase in the overall heat load requirement. However, an increase in the number of stages below the side reboiler by four stages returns the overall heat load to the original value (Column *c*). With the increased number of stages, the driving force distribution above the side reboiler for Columns *a* and *c* is similar. Finally, the use of a very large number of stages below the side reboiler maximises the heat load of the side reboiler, with the operating line touching the equilibrium line at the side reboiler stage (Column *d*)

The conclusion is that the positioning of a side exchanger in an actual distillation column will either increase the overall heat load or the required number of stages (or a combination of both), due to the requirement to keep feasible driving forces for separation through the column.

The correct identification of opportunities to implement side exchangers, with respect to both location and heat load, has therefore to consider the distribution of driving forces in the column, a point that has not been addressed by the traditional reversible column models.

Several methodologies for improved design of distillation columns by using driving-force distribution analysis have been proposed. One approach is the diabatic distillation column, where heat is added and withdrawn by heat exchangers on each tray (Rivero, 2001). In this column, the correct choice of intermediate heat load and utility temperature leads to a much improved distribution of driving forces, and overall better 2nd Law energy efficiency (de Koeijer et al., 2002a, 2002b, 2004; Røsjorde and Kjelstrup, 2005). Driving force is described by entropy production rates, and numerical procedures are used to compute the optimal distribution leading to minimum entropy production.

Another approach is the *internal heat-integrated distillation column* (HIDIC) (Nakaiwa et al., 2003; Gadalla et al., 2005; Iwakabe et al., 2006), where part (or the whole) of the rectifying section is heat-integrated with part (or the whole) of the stripping section, through the use of a higher pressure in the rectifying section (compared to the stripping section pressure) and a number of heat exchangers. This concept makes use of the heat available in the rectifying section to satisfy the heat requirement in the stripping section. Most research work was developed using the separation of binary system. More recently Iwakabe et al. (2006) studied a heat-integrated column separating a multicomponent mixture.

While both the HIDIC and diabatic column concepts improve the energy efficiency of the distillation process, their implementation in practice requires a rather complex column, with many intermediate heat exchangers.

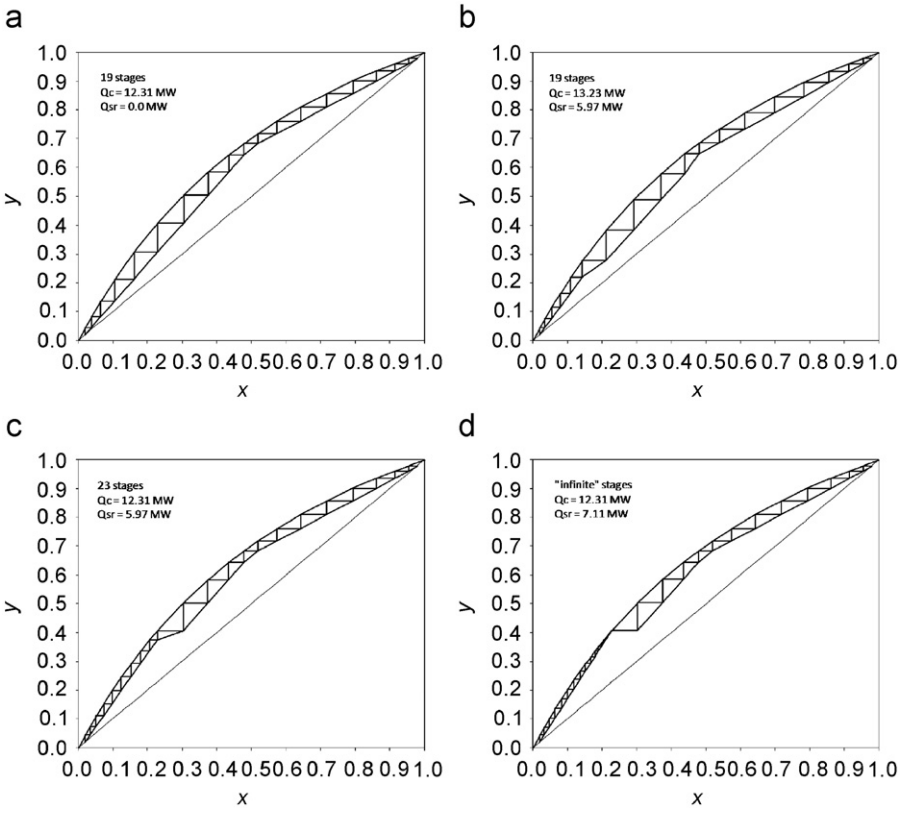

Fig. 3. Composition diagram for different column configurations, with fixed number of stages: (a) no side reboiler; (b)–(d) different side reboiler loads.

However, the suitable positioning of a small number of heat-exchangers in a distillation column, and the implications on energy requirement and column modifications, are still not properly addressed.

2. Minimum driving force in process design

Ideal processes have no driving forces but they can never be realised in practice. Any real process needs some potential difference, a driving force, to be feasible.

The driving force affects both the size and thermodynamic efficiency of the equipment in question. As the driving force approaches zero the unit becomes more reversible and hence thermodynamically more efficient, but at the same time the size of the equipment, and hence its capital cost becomes infinite. Also, the driving forces, however measured, in different unit operations might have differing impacts on the overall process economics.

In process design it is common practice to define a minimum driving force to guarantee feasibility and a good capital-energy trade-off. For example, in the design of heat exchanger networks the temperature difference between the streams is the driving force. So a minimum approach temperature is chosen for the design, the ΔT_{min}. Based on this temperature difference, energy and area targets for heat integration can be established by constructing the composite curves from the process material and energy balances. The composite curves determine the minimum process utility requirement for a given minimum approach temperature (Smith, 2005).

When the composite curves just touch, there is no driving force for heat transfer at some point in the process, which would then require an infinite heat transfer area and hence infinite capital cost. As ΔT_{min} is changed from a small to a large value, the capital cost decreases, but the energy cost increases. When the two costs are combined to obtain the total cost, the optimum point in the capital/energy trade-off is identified, corresponding with the optimum value of ΔT_{min} (Fig. 4).

Fig. 5 shows the composite curves when an intermediate hot utility is placed in the process. In Fig. 5a, the overall heat load of the process is kept constant (as is the ΔT_{min}), and the decrease of temperature difference due to the new utility will require an increase in heat exchanger area. In Fig. 5b, the composite curves are shifted apart to reduce area requirement (by increasing the driving force ΔT_{min}), but at the cost of an increase in the utility consumption.

This is very similar to the observations made previously for the positioning of a side reboiler in a distillation column. In both cases the excessive decrease in driving force is counterbalanced by an increase in overall heat load.

However, while in heat exchanger network design the temperature difference ΔT_{min} can easily be established as the driving force, the identification of an appropriate driving force for distillation processes is not so straightforward.

3. Driving forces in a distillation process

Any methodology to estimate correct heat load targets will require consideration of the available driving forces. In a distillation tray the true driving force for mass transfer is the chemical potential between the two phases. For heat transfer it is the temperature difference between the two phases. These differences lead to the exchange of heat and/or mass. Chemical potential, however, is difficult to calculate. It is defined for each component in each phase and results in a large set of variables, especially for multicomponent systems. It is difficult to define an overall mass transfer driving force based on chemical potential to describe mass transfer for all components. In addition, chemical potential is not as intuitive a driving force as temperature or pressure difference.

A driving force based on composition difference has been proposed by Gani and Bek-Pedersen (2000). However, this approach requires the choice of key-components, and as only equilibrium data are required (for the case of distillation), will not show the distribution of driving force under different column configurations. Also, this approach does not account for heat transfer driving forces that are inherent to distillation.

A more convenient choice of driving force in a distillation tray is obtained by considering that processes occurring with finite driving forces are irreversible, and therefore lead to a loss of opportunity to perform useful work, incurring exergy loss. The exergy loss at a tray can easily be calculated (see Appendix A) and has the advantage of describing the driving forces for multi-component heat and mass transfer in a single variable as it reflects the differences in temperature and composition across the tray.

To illustrate how exergy loss relates to driving force, consider the placement of a side reboiler in a binary column, as shown

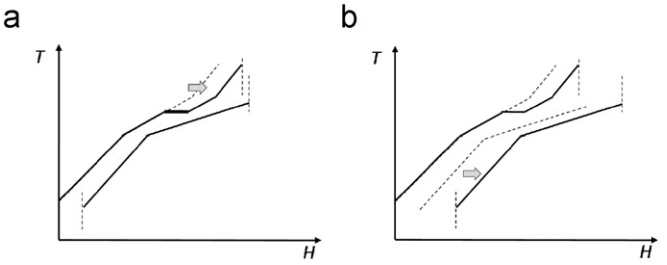

Fig. 5. Placement of intermediate utility and effect on driving forces: (a) decrease in driving forces due to an intermediate utility and (b) increasing driving forces by increasing overall heat load.

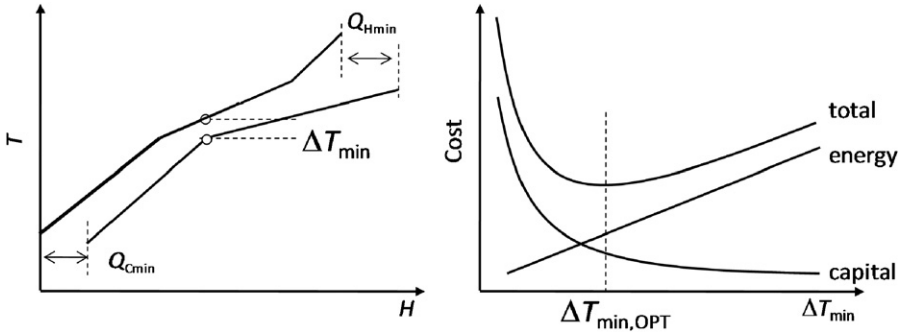

Fig. 4. Minimum driving force for heat exchanger networks.

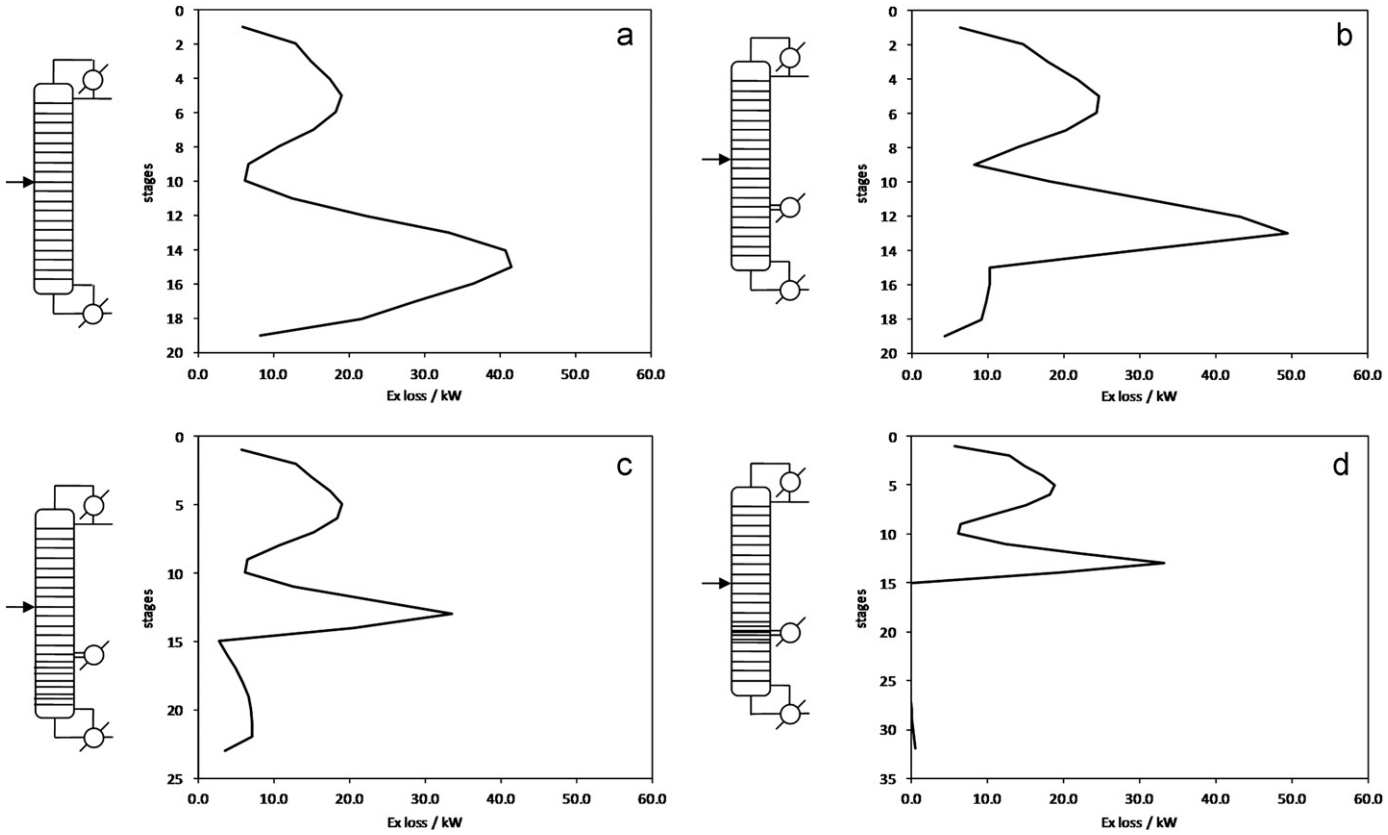

Fig. 6. Exergy loss profile for: (a) simple column, (b) column side reboiler, (c) column with side reboiler and added stages, and (d) column with maximum side reboiler heat load and infinite stages.

previously. The placement of a side reboiler reduces the driving forces in the section near the side reboiler, at the expense of an increase in driving forces above the side reboiler (shown in Fig. 3b). A similar behaviour can be identified in the Exergy Loss Profile (Zemp, 1994) for this column, as shown in Fig. 6b. The positioning of the side reboiler at Stage 14 clearly reduces the exergy losses below the side reboiler, but increases the exergy losses above the side reboiler.

The increase of number of stages (Fig. 6c) returns the exergy losses at the section above the side reboiler to the original values (profiles above Stage 14 in Fig. 6a and b are the same), while still reducing the exergy loss below the side reboiler.

As the side reboiler load increases, the exergy losses in the section between the side reboiler and the main reboiler decrease until the maximum heat load (Q_{max}) is reached and a pinch is formed. At the pinch, the driving forces, and hence the exergy loss, are zero and the column would require an infinite number of stages (Fig. 6d).

Most of the research work in the past focused on determining Q_{max}, the maximum heat load. However, a side exchanger duty can be determined so as to achieve a given minimum diving force, $Ex_{loss,min}$, as illustrated in Fig. 7. Because a minimum driving force is used, the specified side exchanger duty could lead to a feasible and practically achievable design with a finite number of stages.

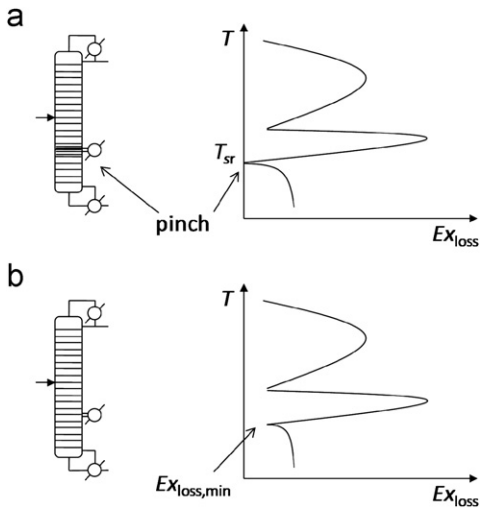

Fig. 7. Targeting the side exchanger heat load with a minimum driving force: (a) pinched column and (b) column with minimum exergy loss.

3.1. Determination of the minimum exergy loss

In theory, as in the case of ΔT_{min} in heat exchanger networks, any value can be used to define $Ex_{loss,min}$. $Ex_{loss,min}$ can be set based on previous experience or can even be determined by economic optimisation. However, a closer analysis of how distillation columns are designed can help to identify an appropriate value for $Ex_{loss,min}$.

The starting point for the design of a distillation column is the choice of an appropriate ratio of reflux to minimum reflux. By analogy to heat exchanger networks, too low a reflux ratio will lead to a very large number of stages.

The final optimum reflux ratio (R_{opt}) for an actual distillation column is obtained by performing a detailed capital-energy trade-off. However, at early design stages simple distillation columns

(with no side exchangers) are designed with a value of R_{opt} around 1.1 times the minimum reflux ratio, as this leads to design configurations close to the optimum final design. Because actual distillation columns operate at a reflux above the minimum reflux value, they already incorporate a minimum driving force, leading to a finite number of separation stages (instead of infinite number of stages, for a minimum reflux column).

An assumption can now be made where the modified column with additional exchangers should operate with at least the same minimum driving force as of the base case column. The rationale behind this assumption is that by maintaining the minimum driving force (of the modified column) similar to the minimum driving force of the base case design, the balance between capital and energy is maintained. This existing driving force just needs to be interpreted in terms of exergy loss so that it can be used to target side reboiling/condensing.

For binary systems the minimum exergy loss (apart from the condenser and reboiler stages, where the loss tends to zero) is usually located at the feed stage (Zemp, 1994), as shown in Fig. A.1 (Appendix A), and can thus be used as the minimum driving force for side reboiling/condensing. Once $Ex_{loss,min}$ has been defined it can be used to determine the side exchanger heat load (Q_{target}) so as to obtain $Ex_{loss,min}$, as shown in Fig. 8. The side reboiler heat load target is the side reboiler duty that achieves $Ex_{loss,min}$ at the stage immediately below the side reboiler. For side condensing, $Ex_{loss,min}$ would be reached at the stage immediately above the side condenser.

For multicomponent separations the exergy profile normally shows a peak of exergy loss at the feed stage, due to the unavoidable mixing losses caused by temperature and composition mismatches between the feed stream and the column streams at the feed stage. However, a minimum exergy loss ($Ex_{loss,min,feed}$) around the feed stage can still be identified above or below the feed stage (Fig. 8a).

Unlike binary systems, for multicomponent systems the minimum exergy loss around the feed stage does not necessarily set $Ex_{loss,min}$. The reason is that, for multicomponent systems, as the side exchanger duty increases, a minimum in the exergy loss might be formed some stages away from the side exchanger (Fig. 8b). Increasing the heat load further reduces this minimum (Fig. 8c), but without any significant reduction in the section exergy loss. Extra stages only cause the formation of a pinch without any significant benefit (Fig. 8d).

The problem of the addition of a large number of stages can be avoided by identifying the minimum at its early stage of formation, and use this exergy loss, $Ex_{loss,min,sr/sc}$, as the minimum driving force. $Ex_{loss,min,feed}$ is not always lower then $Ex_{loss,min,sr/sc}$, as it depends on the particular separation and also on the stage under consideration. $Ex_{loss,min,sr/sc}$ tends to be higher towards the feed stage, and lower than $Ex_{loss,min,feed}$ towards the condenser and the reboiler.

4. The minimum driving force profile

Once a minimum driving force in distillation processes has been established a procedure can be proposed to obtain feasible side exchanger heat load targets. The objective is to identify the side exchanger heat load and additional stages required for the column, while satisfying the following conditions:

- The overall heat load of the column is maintained constant, that is, the addition of a side exchanger should not modify the energy balance of the column (apart from the temperature of the side exchanger utility).
- The modified column must achieve the original desired separation specification.
- No stage should operate with an exergy loss lower than the chosen $Ex_{loss,min}$.

A procedure can then be proposed that computes rigorously the heat load targets.

4.1. Calculation algorithm

Given a converged column simulation, the algorithm for computing the minimum driving force profile is:

1. Define the value of the acceptable minimum driving force, $Ex_{loss,min}$.

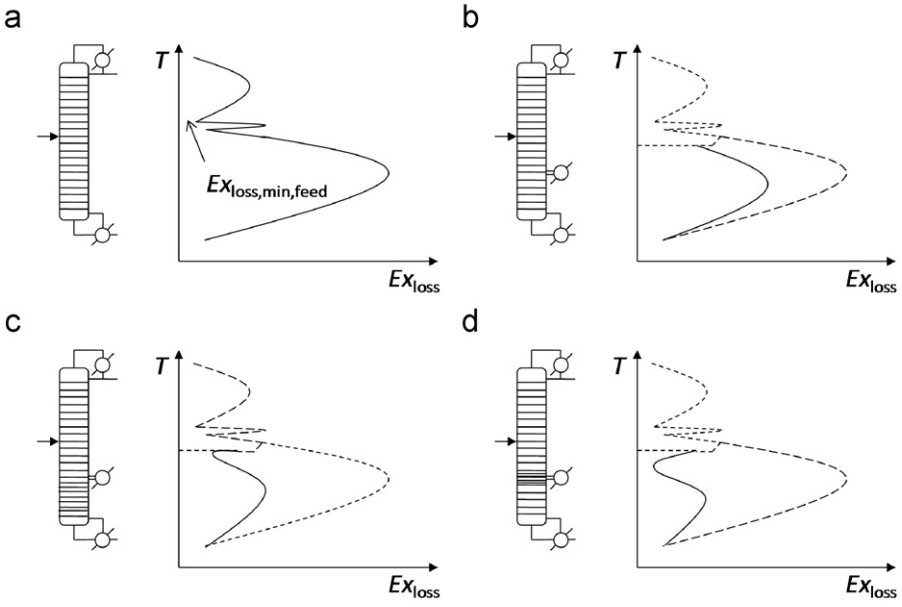

Fig. 8. Pinch formation in multicomponent systems.

2. For each Stage m in the stripping section of the original column:
   a. Add one stage at the bottom of the column.
   b. Place a side reboiler at Stage m and compute the heat load that maintains the overall energy requirement constant, while satisfying product purity and component recovery specifications.
   c. Compute the exergy loss profile and identify the stage around the side reboiler or below the side reboiler where the minimum exergy loss occurs.
   d. If minimum exergy loss is equal to the chosen minimum driving force, or the formation of a minimum in the exergy loss profile is detected, the computed heat load is the heat load target. If not, return to Step a.
3. Repeat the procedure for each Stage m of the rectifying section of original column, increasing the number of stages at the top.
4. Combine the heat load targets for all stages of both sections to obtain the minimum driving force profile (MDF profile).

This procedure involves solving rigorously heat and mass balances for each stage in the column and can be implemented either in a commercial column simulator, or by developing a computer programme. However, this procedure can be significantly simplified after examining the effect of the side exchanger in the column (Soares Pinto, 1999).

The main effect of placing a side reboiler, for example, is to change, relative to the corresponding simple column, the vapour and liquid traffic in the section between the side reboiler and the main reboiler. As a result, the driving forces in this section are smaller than in the base case. In the section above the side reboiler, however, the flows remain essentially the same as in the base case, as the reflux ratio has not changed. This section can in this way be isolated from the main column, thus obtaining a reboiled absorber with a side exchanger, with the flows and composition in and out of the absorber being those of the base case column.

However, small changes in flows and compositions are expected for multicomponent systems in the stages above the side reboiler, and therefore a small number of stages above the side reboiler must be included in the reboiled absorber to allow return to the base case compositions (Fig. 9).

The feed flow rate and composition to the reboiled absorber are given by the liquid entering the m–k–1 stage of the main column, where m is the stage where the side reboiler is intended. The k stages above the side reboiler are there to take into account the effect of the side reboiler on the composition of the vapour leaving the side reboiler. The value of k is chosen to meet the desired accuracy, but a higher value increases the computation time to solve the absorber. Typically, $k=2$ has been shown to lead to acceptable results.

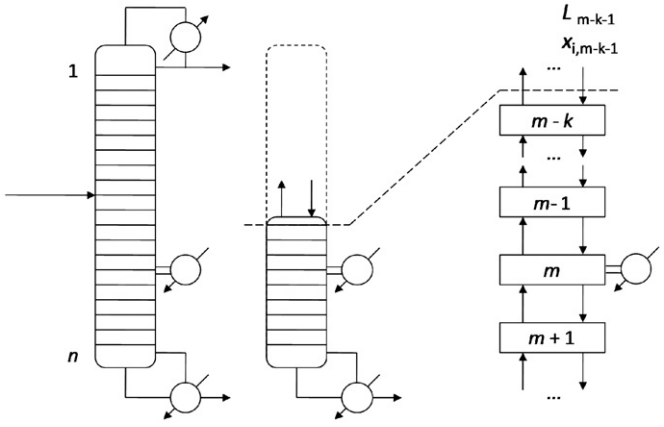

Fig. 9. Reboiled absorber model for side reboiling.

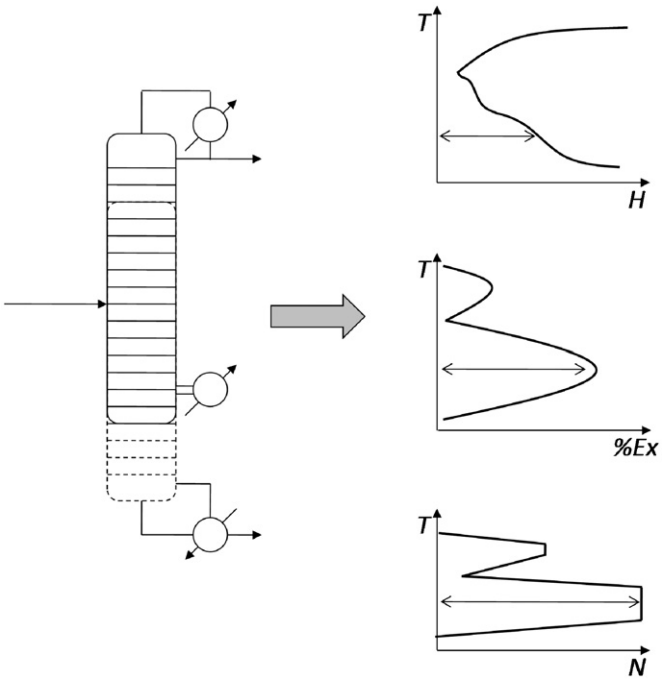

Fig. 10. Minimum driving force profiles: heat load targets, exergy savings, and addition stage requirement.

In the case of a side condenser at stage m, the section between the side condenser and the main condenser can be modelled as a refluxed absorber by analogy.

The refluxed and reboiled absorber models make the calculation procedure much simpler and faster and are the basis of the calculation algorithm implemented in this work. The mass, energy and equilibrium equations for the reboiled and reflux absorber can be solved by a variety of methods (Kister, 1992; Seader and Henley, 2006), among them the bubble-point method of Wang and Henke (1966), suitable for narrow-range boiling systems. This method employs a tridiagonal matrix for the solution of the mass balance equations for a given temperature and vapour profile in the column. In each iteration a new set of temperature and vapour flows is found using bubble-point and energy balance equations.

The final result of the proposed procedure is the heat load target curve for the distillation column, which allows for the identification of the side exchanger heat load targets along the column, as shown in Fig. 10 (top).

4.2. Determining the appropriate location for a modification

The result of the minimum driving force profile procedure is a target of the side exchanger heat load for every stage in the column. Another important issue for column design/optimisation is the determination of the best location to place the side exchangers.

Each of the heat load targets will have a different impact on the column thermodynamic efficiency, and since exergy reflects the quality of the heat required or rejected by the column, the exergy required to accomplish the desired separation. This exergy requirement is fulfilled by the heat flow from and to the utilities, and can be computed by

$$Ex_{\text{exchanger}} = Q_{\text{exchanger}}\left(1-\frac{T_0}{T_{\text{ideal utility}}}\right)$$

where the temperature of the 'ideal' utility is taken to be that of the stage, i.e., the exergy loss due to heat transfer between the utility and the stage is not considered.

The "utility exergy requirement" of the base case is then defined as

$$Ex_{base} = Ex_{reb,base} + Ex_{cond,base}$$

The heat load targets obtained from the minimum driving force profile can be used to compute the utility exergy requirement for the modified column. The required utility exergy is given by the exergy needs of the original and modified reboiler and condenser, and of the side exchangers:

$$Ex_{mod} = Ex_{reb,mod} + Ex_{cond,mod} + \sum_j Ex_{side}$$

The exergy savings of allocating a side exchanger at a given stage can so be expressed by

$$\%\ \text{savings in utility exergy} = 1 - \frac{Ex_{mod}}{Ex_{base}}$$

The values of the exergy savings for each stage can be plotted as a function of the stage location or stage temperature to obtain the Savings in Utility Exergy Profile (SUEP), as also shown in Fig. 10 (middle). The SUEP establishes the best location to place a side reboiler/condenser from a column thermodynamic point of view, i.e. for minimum exergy loss for the separation, and with the assumption of ideal utilities being used to satisfy heating and cooling requirement.

The proposed procedure also targets the number of additional stages required to achieve $Ex_{loss,min}$ in the column (Fig. 10, bottom).

If utility costs or heat recovery opportunities have been taken into account, the best side exchanger location would change: it would be at the temperature corresponding to the utility or recovered heat and its duty would be given by the minimum driving force profile. Note that the minimum driving force profiles provide a set of design options: for each proposed side exchanger stage, the benefits in terms of exergy loss, the side exchanger duty and the number of additional stages are computed. This set of solutions allows designs alternatives to be evaluated with respect to both thermodynamic and economic performance, taking into account capital-energy trade-offs.

5. Examples

Three examples are used to demonstrate the feasibility of the proposed methodology, including a binary system, a ternary and a 5-component system. The objective is to show that minimum driving force profiles can identify feasible side exchanger heat load targets.

5.1. Example: binary system

The first example is a binary system, where the reversible column profile can easily be obtained. The separation specifications are shown in Table 1. The column was designed by selecting the number of stages such that the ratio of R/R_{min} was 1.25 and the feed stage location minimised the condenser duty. The column has 26 stages (including the total condenser and reboiler), with feed located at stage 13. The simulation results using HYSYS are shown in Table 2.

The reversible column profile for this separation is shown in Fig. 11. There is scope for the use of side reboiling. For example, at a side reboiler temperature of 90 °C a heat load target of 4.9 MW can be identified. Because the heat loads shown on the profile refer to an ideal column with an infinite number of stages, the suggestion by Dhole and Linnhoff (1993) to use 70–80% of the value indicated on the profiles will be considered. So the column was the simulated with a side reboiler located at stage 18, and a heat load of 100% and 75% of the targeted value. The results are summarised in Table 3.

There is a penalty on the overall energy requirement, with an increase of 8.4% (for 100% target) and 5.3% (for 75% target) in hot utility load. More importantly, the temperature of the side reboiler stage has shifted from 90.2 to 95.7 °C (100% target) and 94.4 °C (75% target). Clearly, neither the predicted targets for heat load nor temperature have been achieved. A number of design changes could now be carried out, trying to achieve the desired target values. However, an appropriate choice of side reboiler heat

Table 1
Feed and product specification, binary system.

Feed properties	
Molar flow (kmol/h)	1000
Pressure (kPa)	800
Temperature (°C)	82.8
Vapour fraction	0.0
Molar fractions	
n-butane	0.5555
i-pentane	0.4445
Column specifications	
Top recovery of n-butane	0.98
Bottom recovery of i-pentane	0.98
Physical properties	
Peng–Robinson equation of state	

Table 2
Simulation results, binary system.

Stage	Exchanger	T/°C	Q/MW
1	Condenser	70.0	10.05
26	Reboiler	104.0	10.24

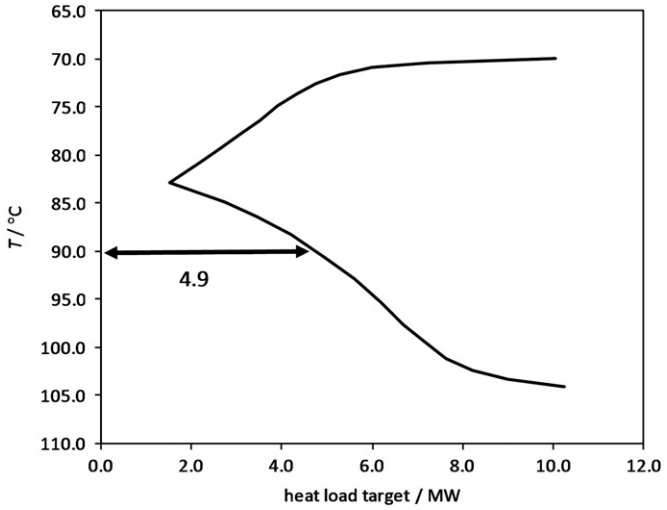

Fig. 11. Heat load targets using the reversible column methodology.

Table 3
Simulation results for reversible targets, binary system.

Target (%)	Q_{side}/MW	Q_{cond}/MW	T/°C
100	4.90	10.89	95.7
75	3.70	10.60	94.3

load and location can only be identified by further simulations and trial and error.

Targets will now be computed using the proposed minimum driving force profile methodology. The exergy loss profile is computed as described in Appendix A, and is presented in Fig. 12.

In Fig. 12 the minimum exergy loss at the feed stage is 3.25 kW. Running the minimum driving force profile algorithm with this value of minimum exergy loss gives the profile shown in Fig. 13. Although the shape is similar to the reversible profile obtained for the same system (Fig. 11), the target values are smaller. At stage 18, with 90 °C, a heat load target of 3.91 MW can be identified, which corresponds to approximately 80% of the reversible profile target. In addition, the methodology predicts that five additional stages should be added below the side reboiler to maintain the original utility load (Fig. 14).

Simulation of the column with the modifications proposed by the minimum driving force procedure shows that that the total heat loads and side reboiler temperature are in excellent agreement with those of the base case simulation (Table 4).

The reasons for the better targeting results using the minimum driving force profiles can be identified by analysing the exergy loss profiles for both cases (Fig. 15). The addition of the heat load predicted by the reversible column approach (Fig. 15a) decreases

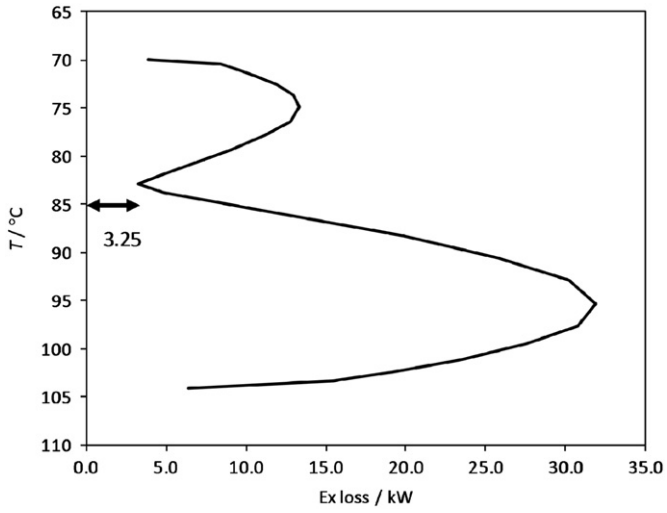

Fig. 12. Binary system: exergy loss profiles.

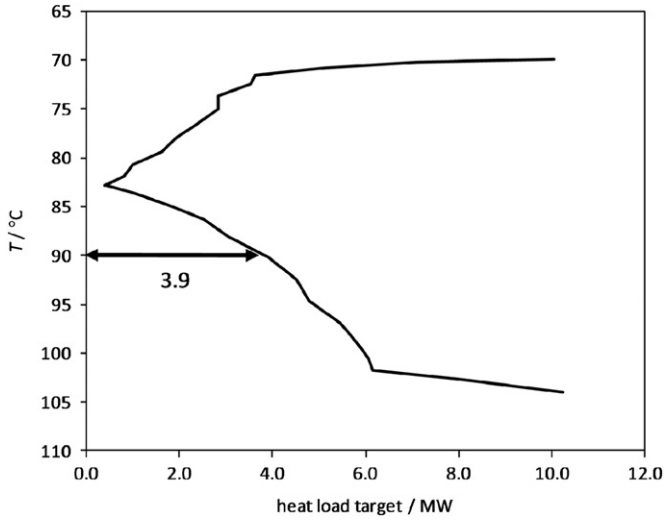

Fig. 13. Minimum driving force plot for $\Delta Ex_{min,loss}=3.25$ kW.

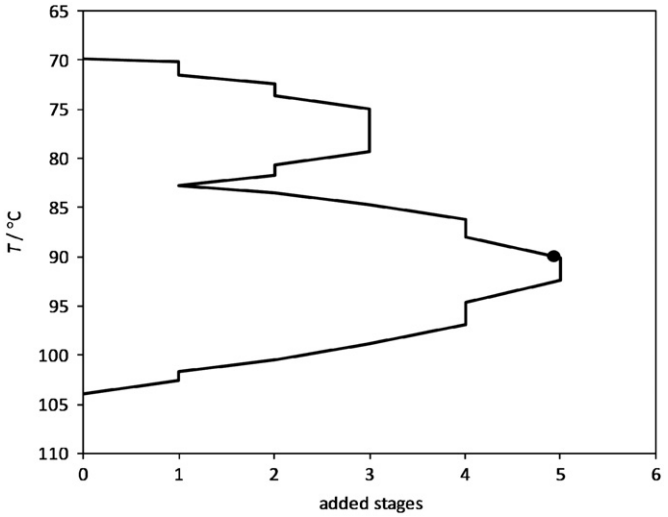

Fig. 14. Stages added for $\Delta Ex_{min,loss}=3.25$ kW.

Table 4
Simulation results, minimum driving force targets, for binary system.

Stage	Exchanger	Base case	Simulation	
		Q/MW	T/°C	Q/MW
1	Condenser	10.05	–	10.04
18	Side reboiler	–	90.3	3.91
31	Reboiler	10.24	–	6.32

the exergy losses in the section below the side reboiler, but due to the fixed number of stages, increases the exergy loss in the column section above the side reboiler. Overall, there is a shift of exergy losses from the bottom of the column to the top of the column, and the increase in driving forces in the top section. Here, due to the fixed number of stages, an increase in liquid and vapour traffic is required, increasing the condenser heat load.

On the other hand, in the minimum driving force design the exergy loss distribution remains unchanged in the column section above the side reboiler, and a much higher reduction of exergy losses is achieved between the side reboiler and the main reboiler (Fig. 15b). The minimum driving force design results in greater reduction in exergy loss than the reversible design without creating additional exergy losses in other sections of the column.

5.2. Example: ternary system

In this example the minimum driving force methodology is applied to a column separating three hydrocarbons. Table 5 shows the feed and product specifications for this column. The column has a saturated liquid feed and is separating n-butane from i-pentane.

The column has been simulated using HYSYS, with a number of stages selected to operate the column with a ratio of actual reflux to minimum reflux of 1.15 (20 stages), and the feed stage optimised to minimise the condenser duty (feed at stage 11). Table 6 shows the results obtained.

5.2.1. Minimum driving force approach

The exergy loss profile for this column is shown in Fig. 16. As can be observed the column has a large exergy loss in the stripping section compared with the rectifying section, thus indicating a large scope for side reboiling. The minimum driving

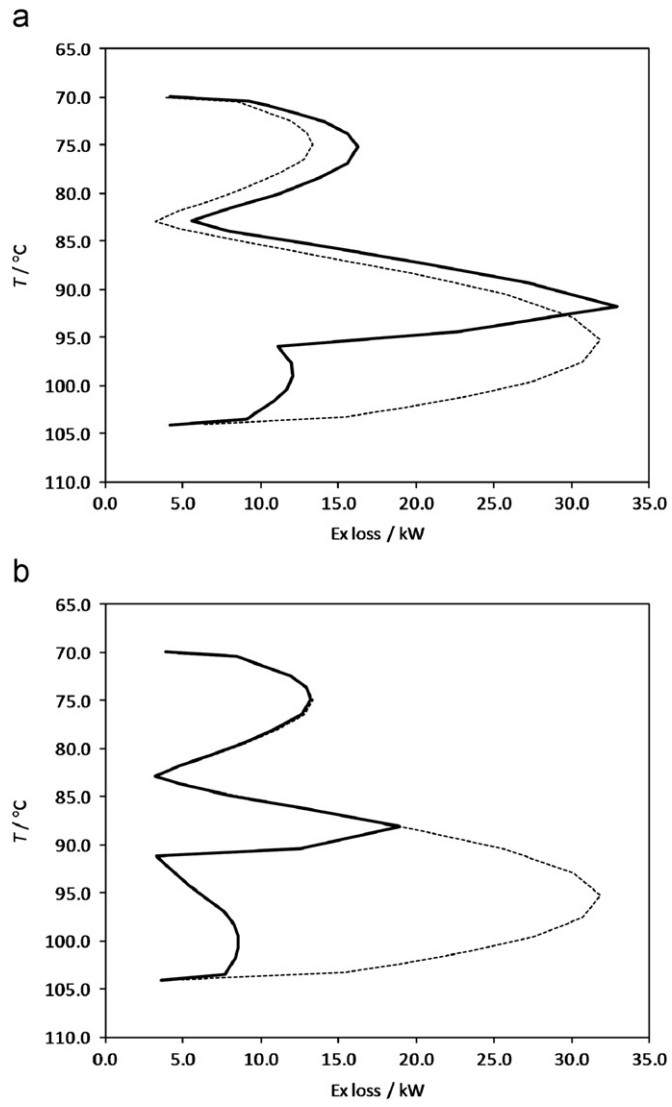

Fig. 15. Exergy loss distribution for: (a) reversible targets, and (b) minimum driving forces (solid line: after modifications; dashed line: base case).

Table 5
Feed and product specification for the ternary system.

Feed properties	
Molar flow (kmol/h)	500.0
Pressure (kPa)	100.0
Temperature (°C)	0.63
Vapour fraction	0.0
Molar fractions	
i-butane	0.333
n-butane	0.334
i-pentane	0.333
Column specifications	
Top recovery of n-butane	0.98
Bottom recovery of i-pentane	0.98
Physical properties	
Peng–Robinson equation of state	

force for this column, given by the smallest exergy loss around the feed stage, is 0.38 kW.

Once the minimum driving force has been set, the minimum driving force profiles are generated. Fig. 17 shows the heat load targets as a function of temperature, and Fig. 18 shows the

Table 6
Simulation results.

Stage	Exchanger	T/°C	Q/MW
1	Condenser	−6.8	3.569
20	Reboiler	26.5	3.665

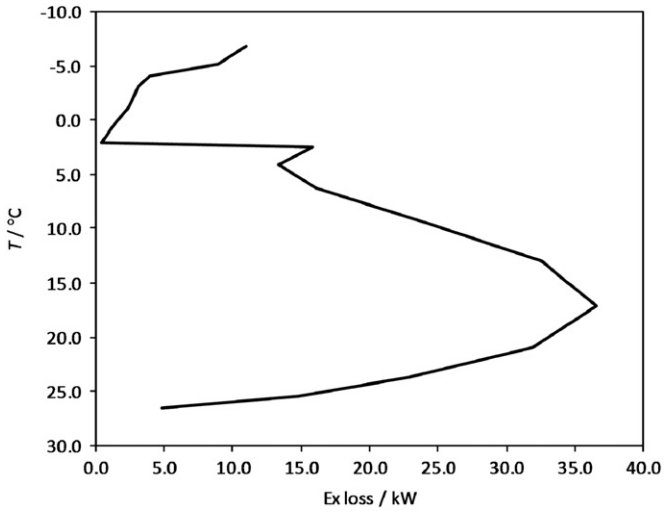

Fig. 16. Exergy loss profile for ternary column.

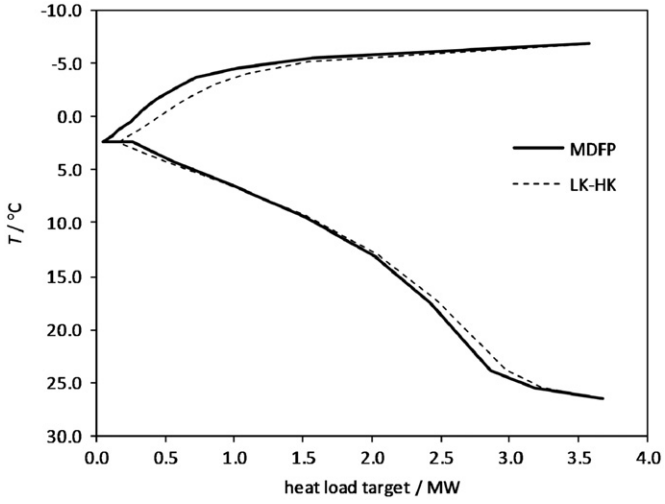

Fig. 17. Heat load targets for ternary column using MDF profile and the LK–HK reversible column methodology.

additional stages required. In order to test the proposed methodology over a range of side reboiler locations four different stages were chosen as shown in Table 7.

Table 7 shows the simulation results after placing the side reboiler at the four positions. As can be observed, the simulation results are in complete agreement with the targets established previously. There are negligible penalties in the overall utility consumption (up to +0.2%) and temperature shift (maximum of 0.3 °C) therefore avoiding the need for additional simulations.

5.2.2. *Reversible profile approach*

The reversible profile is computed using the light key–heavy key (LK–HK) procedure outlined by Dhole and Linnhoff (1993). The profile obtained by considering n-butane as the light key and

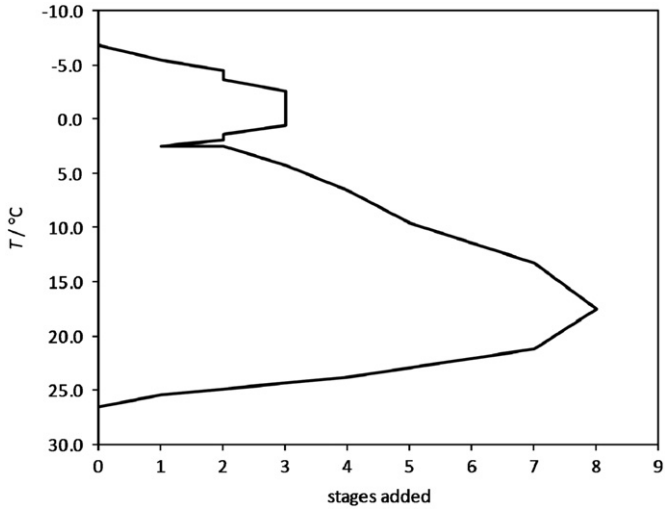

Fig. 18. Stages added for ternary system.

Table 7
MDF profile targets and simulation results for the ternary system (T: temperature of stage with side reboiler; Q: duty of side reboiler).

Stage	MDF targets			Simulation	
	T/°C	Q/MW	+ stages	T/°C	Q_{cond}/MW
0	–	–	–	–	3.570
12	4.2	0.546	3	4.3	3.577
14	9.5	1.511	5	9.5	3.575
15	13.3	2.028	6	13.1	3.573
17	21.2	2.679	7	20.9	3.574

Table 8
LK–HK profile targets and simulation results for the ternary system (T: temperature of stage with side reboiler; Q: duty of side reboiler).

Stage	MDF targets	Simulation			
	Q/MW	100% LK–HK targets		75% LK–HK targets	
		ΔT/°C	Q_{cond}/MW	ΔT/°C	Q_{cond}/MW
0	–		3.57	–	3.57
12	0.546	+1.2	3.64	+0.8	3.61
14	1.511	+4.4	3.67	+3.0	3.63
15	2.028	+5.6	3.68	+3.7	3.64
17	2.679	+3.1	3.66	+1.9	3.61

i-pentane as the heavy key is shown in Fig. 17, together with the minimum driving force profile. For this example both profiles have a similar shape. As the near-reversible targets are very similar to the minimum driving force targets, columns using the heat load targets predicted from the minimum driving force profile were simulated to verify the LK–HK approach, again using 100% and 75% of the target values. The results are shown in Table 8. For all side reboilers there is an increase in the stage temperature (up to 5.6 °C) and overall column heat load (up to 3% in condenser duty). Although the use of 75% of the target value reduces the penalty in temperature and overall heat load, further simulations would still be required to identify the side reboiler location and load that gives the greatest process improvements.

Table 9
Feed and product specification for the five component system.

Feed properties	
Molar flow (kmol/h)	1000
Pressure (kPa)	400
Temperature (°C)	24.95
Vapour fraction	0.4
Model fractions	
Propene	0.1
Propane	0.2
i-butane	0.4
n-butane	0.2
n-pentane	0.1
Column specifications	
Top recovery of n-butane	0.995
Bottom recovery of n-pentane	0.995
Physical properties	
Peng–Robinson equation of state	

Table 10
Base case simulation results for the five component system.

Stage	Exchanger	T/°C	Q/MW
1	Condenser	−8.10	5.90
29	Reboiler	37.87	3.96

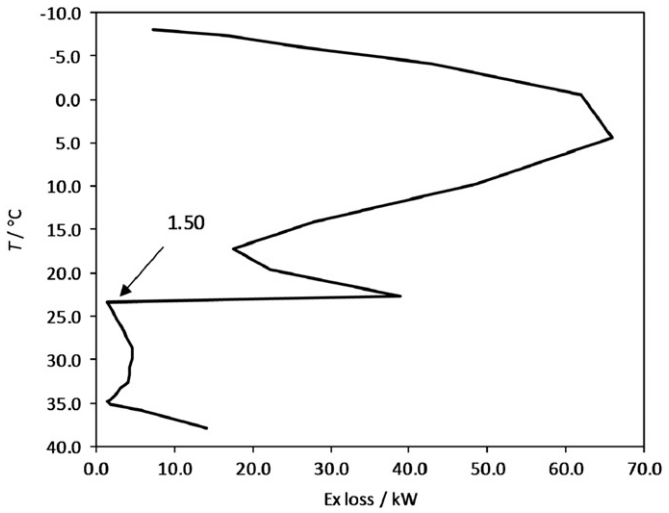

Fig. 19. Exergy loss profile for the five component system in example 3.

5.3. Example: a five-component system

The last example is a five-component system, the feed and product specifications of which are shown in Table 9. The column has 29 stages, and feed is located at stage 11. Table 10 shows the heat load and temperatures of condenser and reboiler of this column.

Fig. 19 shows the exergy loss profile for this column. Large exergy losses occur in the rectifying section, showing scope for side condensing. The exergy loss profile shows a minimum exergy loss around the feed stage of 1.50 kW.

The analysis of the minimum driving force profiles, obtained by using the proposed procedure, lead to the following conclusions:

- The best placement of a side condenser, with respect to utility exergy, is at temperatures around 10 °C, where an ideal utility

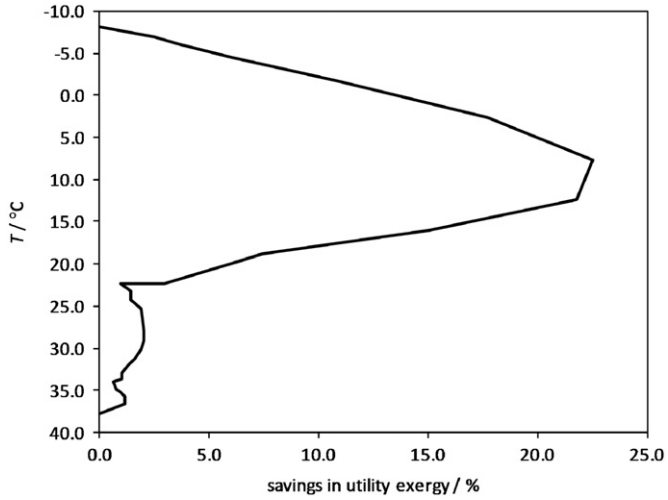

Fig. 20. Savings in utility exergy for the five component system.

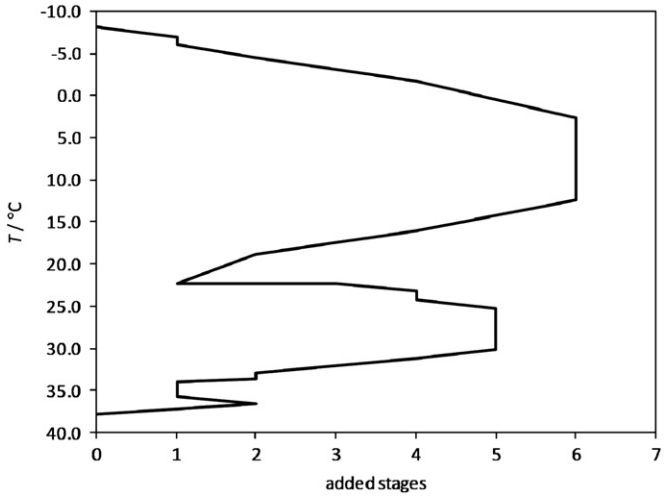

Fig. 22. Added stages for the five component system.

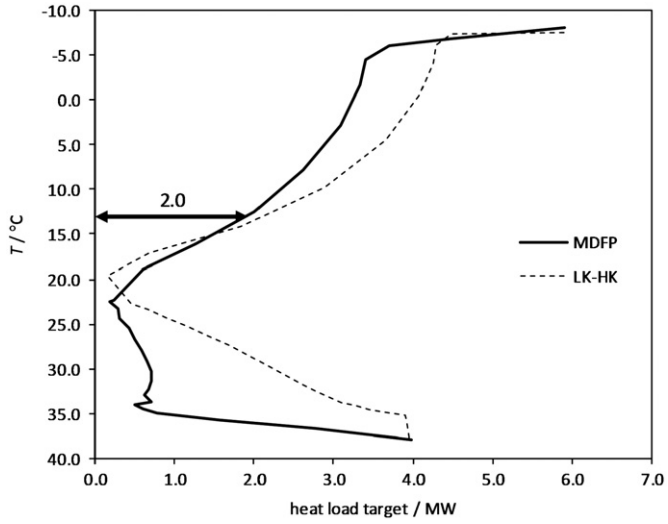

Fig. 21. Minimum driving force profile for the five component system.

exergy saving of 22% can be achieved (Fig. 20). At this temperature the use of chilled water in the side condenser could be suitable (Fig. 21). The stage with a temperature closest to 10 °C is stage 8, with $T=12.5$ °C. At side condenser stage temperature of 12.5 °C a heat load of 2.0 MW can be rejected (Fig. 21).

- Six additional stages are required between the condenser and the side condenser (Fig. 22).

The modified column was simulated with a total of 35 stages, feed at Stage 17 and the side condenser located at the stage with the temperature closest to 10 °C (now Stage 14, was Stage 8 in the base case column).

The results of the simulation of the column with the target values are shown in Table 11. The overall column heat load has remained the same, with a side condenser stage temperature of 12.9 °C. The predicted targets were achieved without further simulation.

On the minimum driving force diagram the near-reversible profile based on key components is also shown (Fig. 21). Clearly, the LK–HK profile over-predicts heat duty targets over almost the whole column (apart from a small section near the feed stage). As in the previous examples, using target values from the LK–HK profile would increase the overall heat duty of the column and shift the side condenser temperature. This effect is particularly pronounced above 25 °C, where LK–HK profile wrongly shows a large scope for side reboiling.

Table 11
Simulation results for side condenser for the five component system.

Stage	Exchanger	Base case	Simulation	
		Q/MW	T/°C	Q/MW
1	Condenser	5.90	–	3.92
14	Side condenser	–	12.9	2.000
35	Reboiler	3.96	–	3.97

6. Comparison with rigorous near-reversible profiles

For the examples shown above, the new column profiles were compared to the near-reversible column profile proposed by Dhole and Linnhoff (1993). These 'near-reversible profiles' (NRP) were obtained by choosing appropriate key-components and then following the procedure for binary systems. Therefore the near-reversible column profile does not provide rigorous results.

An alternative is to compute rigorous profiles following the procedure proposed by Koehler et al. (1991). In this procedure the reversible sections are computed rigorously by solving the multi-component mass and equilibrium equations, and no assumption about key components needs to be made. These profiles are as reversible as possible for the given separation, and are shown in Fig. 23 for the ternary and 5-component systems. The profile section with the constant heat load (dashed vertical line) corresponds to the adiabatic section between the two column pinch points. Although there is a certain similarity between the profiles, the near-reversible curves still differ from the minimum driving force profiles. Furthermore, the near-reversible profiles show column sections with smaller targets than the minimum driving force profiles, an unexpected result considering that the near-reversible distillation (NRD) profiles are obtained under the most reversible conditions.

One reason why near-reversible profiles are not suitable for the correct targeting of side exchanger heat load is that they were obtained for reversible conditions, with no driving forces (apart from the feed section). The other reason is that the near-reversible profiles are a function of feed and product specifications only, and therefore the actual column configuration

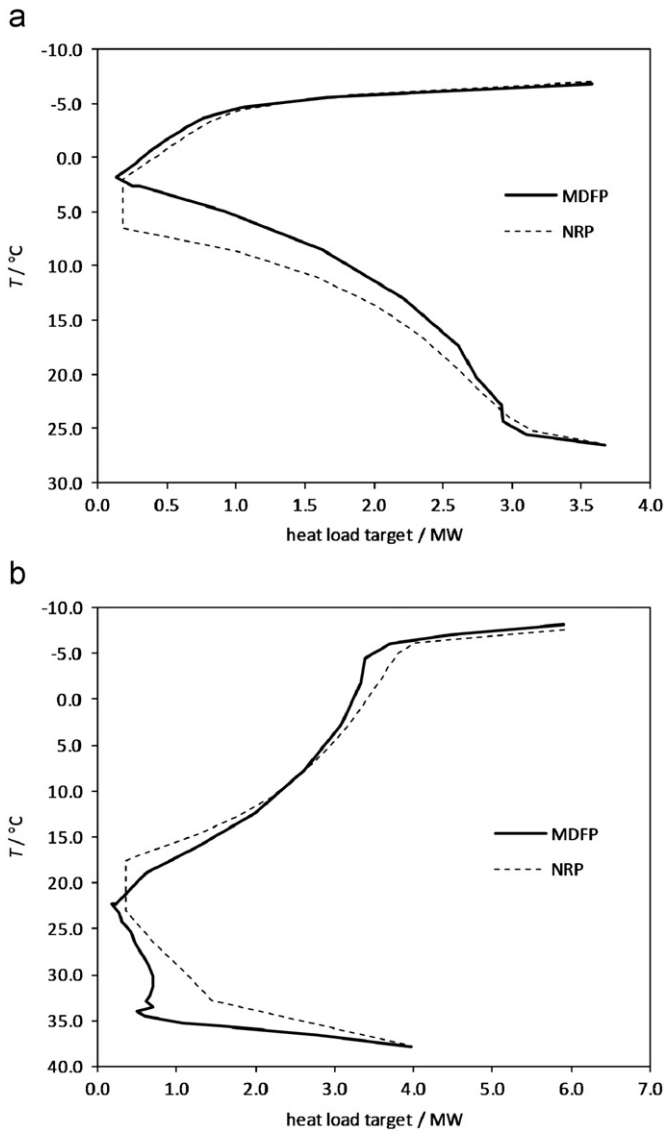

Fig. 23. Comparison between MDF and near-reversible profiles (NRP) (top: ternary system; bottom: 5-component system).

(reflux ratio, feed stage location) is not considered. This is partly overcome by the LK–HK profiles, where the composition profile of the actual column is used in the procedure to obtain the heat target profile. However, reversible behaviour at each stage is still assumed, and strong simplifying assumptions are made to compute the heat load profiles.

One final point should be noted about the profiles compared in Fig. 23. In some regions the near-reversible and minimum driving force profiles cross each other. Near-reversible column profiles can overestimate or underestimate the duty that can be achieved for a side reboiler or side condenser in a real column. That is, using near-reversible column profiles can be misleading when attempting to derive design features for a real column.

7. Conclusions

In this paper a new approach for the analysis of distillation columns has been developed, resulting in a novel temperature–enthalpy profile for targeting side reboiling and side condensing. The main feature of the proposed methodology is the introduction of a minimum driving force for distillation described in terms of exergy loss distribution of the existing column. The minimum driving force allows for the determination of heat load targets that are both feasible and economic.

The minimum driving force profile can be obtained easily from converged computer simulations and provides targets which do not result in heat load penalties or temperature shift therefore avoiding the need for further simulations. In addition to providing realisable targets, the new approach also provides the design engineer with information about the best location to place a side exchanger.

Compared with the more established key-components approach, the new technique has two distinct advantages. Firstly the targets shown on the minimum driving force profile are realisable, in contrast with the light key–heavy key targets, which require additional simulation time and experienced judgement due to heat load penalties and temperature shifts. Secondly, the minimum driving force targets result in column designs which are thermodynamically more efficient and economic, as balancing the benefit of side exchanger load against the penalty of additional stage requirements can be explored at the targeting stage.

The incorporation of a minimum driving force in the calculation of the temperature–enthalpy profile allows appropriate consideration of the available driving forces in the actual column, therefore leading to feasible heat load targets. In contrast, both the key-component approach and the rigorous near-reversible approach are based on the reversible column model; thus they do not correctly identify feasible column modifications. Results shown in this paper lead to the general conclusion that column profiles based on the concept of minimum driving forces, defined in terms of exergy losses, are useful to indicate heat load and location targets for side exchangers.

Nomenclature

Ex	exergy of stream, kW
H	enthalpy of stream, kW
S	entropy of stream, kW/K
T	temperature, K
Q	heat flow, kW
x, y	liquid, vapour phase composition, mol/mol
L, V	liquid, vapour flows, kmol/s
F, D, B	flows: feed, distillate, bottom, kmol/s
q	feed thermal condition

Greek letters

Δ	difference

Subscripts, superscripts

0	ambient
cond, rebo	condenser, reboiler
D	distillate stream
def	deficit
heat	relative to side reboilers/condensers
i	component
in, out	entering, leaving the column or stage
j	stage
liq, vap	liquid, vapour phase
min	minimum
rect, strip	rectifying, stripping section
stage	relative to a column stage
streams	relative to streams entering and leaving the column
utils	relative to the column utilities
*	equilibrium composition

Appendix A

From the point of view of the Second Law of Thermodynamics, a distillation column can be compared to a heat engine. Work from the utility system (heat fed to the reboiler and rejected at the condenser) is used to produce work of separation. This can be described by the exergy balance (Seader and Henley, 2006):

$$\sum \left(1-\frac{T_0}{T_i}\right) Q_i = \Delta Ex_{\text{streams}} + Ex_{\text{lost}} \tag{A.1}$$

where T_i is the temperature of utility i; T_0 the ambient temperature; Q_i the heat load of utility i; $\Delta Ex_{\text{streams}}$ the exergy change of streams $= Ex_{\text{top}} + Ex_{\text{bott}} - Ex_{\text{feed}}$; Ex_{loss} the exergy loss in the column due to irreversibilities.

The exergy of a stream is given by its enthalpy and entropy as

$$Ex = H - T_0 S \tag{A.2}$$

The irreversibilities in the column are due to the differences of temperature and composition of the streams mixing at the different positions in the column.

The exergy balance can also be applied to each column stage. Here, thermal exergy available from the mixing of the streams entering at different temperatures is used to increase the compositional exergy of the steams leaving the stage. Again, exergy is lost due to the finite temperature and composition differences across each stage. The exergy balance of a stage can thus be expressed as a function of the streams entering and leaving the stage (internal liquid and vapour streams, feed and side streams) and the heat flow to the stage (by a heat exchanger at the stage temperature):

$$Ex_{\text{loss}} = Q_i \left(1-\frac{T_0}{T_i}\right) + Ex_{\text{streams,in}} - Ex_{\text{streams,out}} \tag{A.3}$$

where T_i is the temperature of column side exchanger; Q_i the heat load of side exchanger; $Ex_{\text{streams,in}}$ the exergy of streams entering the stage: $Ex_{\text{vap,in}}$, $Ex_{\text{liq,in}}$, Ex_{feed}; $Ex_{\text{streams,out}}$ the exergy of streams leaving the stage: $Ex_{\text{vap,out}}$, $Ex_{\text{liq,out}}$, $Ex_{\text{sidestream}}$; Ex_{loss} the exergy loss at the stage due to irreversibilities.

Again, stream exergy is computed by Eq. (A.2). Enthalpy and entropy values of a stream can be obtained accurately using

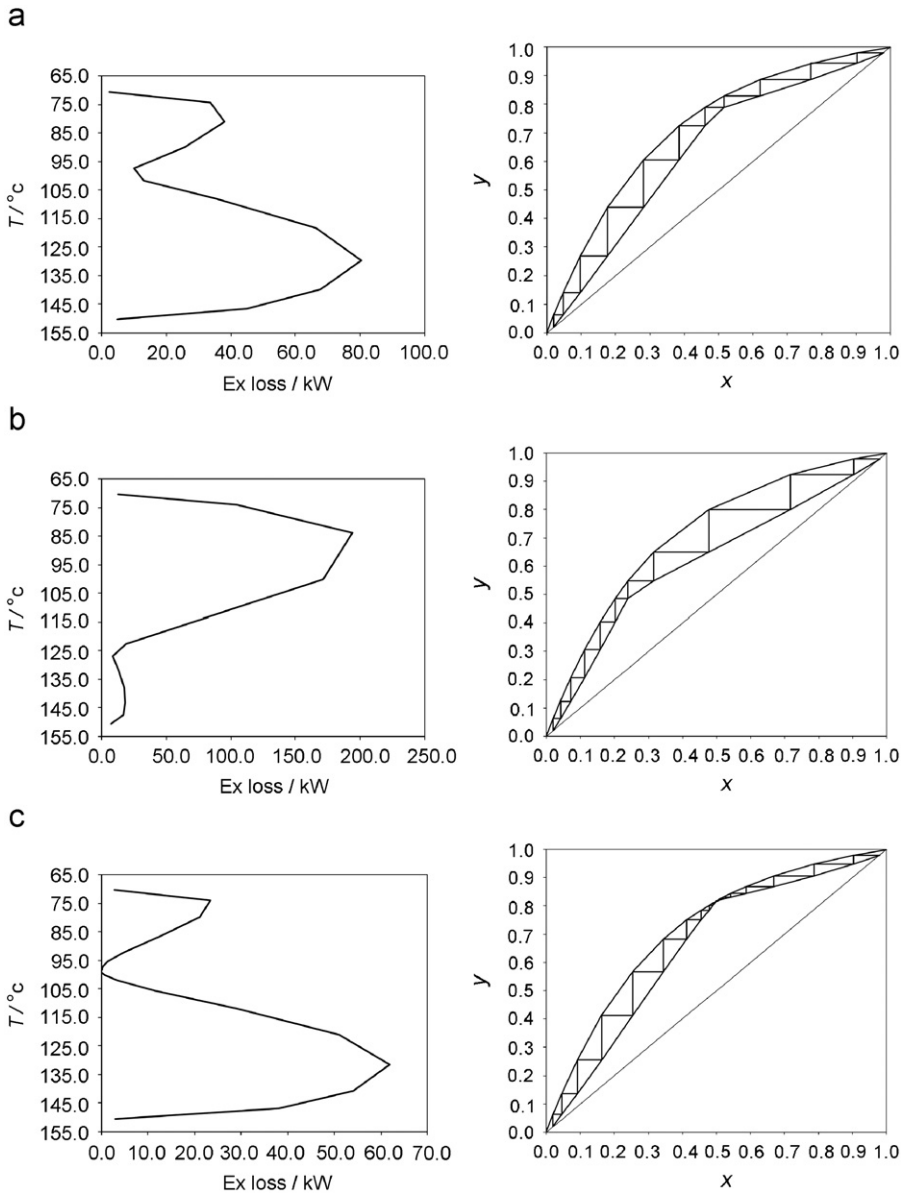

Fig. A.1. McCabe-Thiele diagrams and exergy loss profiles: (a) saturated liquid feed; (b) saturated vapour feed; and (c) minimum reflux.

a commercial simulator, so stage exergy losses can be easily computed from a converged column simulation by applying the exergy balance given by Eq. (A.3). As only compositions, pressure/ and temperatures of the streams entering and leaving a stage are required to compute enthalpy and entropy data, it is not necessary for the column stage to be an equilibrium process. Stage efficiencies or the more recent tray calculations based on irreversible thermodynamics (de Koeijer and Kjelstrup, 2004) can be used if the consideration of equilibrium stage is not appropriate.

The relationship between driving forces and exergy loss can been shown by using the McCabe-Thiele diagram for the separation of a binary mixture, with saturated liquid feed. The exergy loss profile (Fig. A.1a, left) for this column shows large exergy losses in the stripping section, and smaller losses in the rectifying section. On the other hand, close to the top, feed and bottom of the column the exergy losses are small.

Fig. A.1a (right) shows the McCabe-Thiele diagrams for the same column. A comparison of this diagram with the exergy loss profile shows that the distribution of exergy losses in the column is similar to the distance between the operating and the equilibrium line, which is a measure of the driving force at a given stage. Near the top, feed and bottom of the column, both lines are closer than in the intermediate sections, and the average distance in the rectifying section is smaller than in the stripping section.

A similar behaviour can be observed for the column operating under different conditions. Both diagrams are shown for saturated vapour feed in Fig. A.1b, and under minimum reflux in Fig. A.1c, where the infinite numbers of stages at the feed stage is described by a column section without exergy losses. In both cases the exergy loss profile follows closely the distance between equilibrium line and operating line.

The shape of the exergy loss profile has been used to identify appropriate modification of distillation columns, e.g. feed pre-heating, change of feed location and use of side exchangers (Zemp, 1994), and is especially suitable for the analysis for multicomponent systems.

References

Aguirre, P., Espinosa, J., Tarifa, E., Scenna, N., 1997. Optimal thermodynamic approximation to reversible distillation by means of interheaters and intercoolers. Industrial and Engineering Chemistry Research 36 (11), 4882–4893.

Bandyopadhyay, S., Malik, R.K., Shenoy, U.V., 1998. Temperature–enthalpy curve for energy targeting of distillation columns. Computers and Chemical Engineering 22 (12), 1733–1744.

Bausa, J., v. Watzdorf, R., Marquardt, W., 1998. Shortcut methods for nonideal multicomponent distillation: 1. Simple columns. AIChE Journal 44, 2181–2198.

Benedict, M., 1947. Multistage separation processes. Transactions of AIChE 43, 41.

Danilov, R.Yu., Petlyuk, F.B., Serafimov, L.A., 2007. Minimum-reflux regime of simple distillation columns. Theoretical Foundations of Chemical Engineering 41 (4), 371–383.

de Koeijer, G.M., Kjelstrup, S., van der Kooi, H.J., Knoche, K.F., Andersen, T.R., 2002a. Positioning heat exchangers in binary tray distillation using isoforce operation. Energy Conversion and Management 43 (9–12), 1571–1581.

de Koeijer, G.M., Kjelstrup, S., Salamon, P., Siragusa, G., Schaller, M., Hoffmann, K.H., 2002b. Comparison of entropy production rate minimization methods for binary diabatic distillation. Industrial and Engineering Chemistry Research 41 (23), 5826–5834.

de Koeijer, G., Røsjorde, A., Kjelstrup, S., 2004. Distribution of heat exchange in optimum diabatic distillation columns. Energy 29 (12–15), 2425–2440.

de Koeijer, G.M., Kjelstrup, S., 2004. Application of irreversible thermodynamics to distillation. International Journal of Thermodynamics 7 (3), 107–114.

Demirel, Y., 2006. Retrofit of distillation columns using thermodynamic analysis. Separation Science and Technology 41 (5), 791–817.

Dhole, V., Linnhoff, B., 1993. Distillation column targets. Computers and Chemical Engineering 17, 549–560.

Flower, J.R., Jackson, M.A., 1964. Energy Requirements in the separation of mixtures by distillation. Transactions of IChemE 42, 249–258.

Fonyo, Z., 1974a. Thermodynamic analysis of rectification. I. Reversible model of rectification. International Chemical Engineering 14, 203–210.

Fonyo, Z., 1974b. Thermodynamic analysis of rectification. II. Finite cascade models. International Chemical Engineering 14, 203–210.

Franklin, N.L., Wilkinson, M.B., 1982. Reversibility in the separation of multicomponent mixtures. Transactions of IChemE 60, 276–282.

Gadalla, M., Olujic, Z., Sun, L., De Rijke, A., Jansens, P.J., 2005. Pinch analysis-based approach to conceptual design of internally heat-integrated distillation columns. Chemical Engineering Research and Design 83 (8), 987–993.

Gani, R., Bek-Pedersen, E., 2000. Simple new algorithm for distillation column design. AIChE Journal 46 (6), 1271–1274.

Ho, F., Keller, G.E., 1987. Process integration. In: Liu, Y.A., McGee Jr., H.A., Epperly, W.R. (Eds.), Recent Developments in Chemical Process and Plant Design. John Wiley and Sons, New York.

Iwakabe, K., Nakaiwa, M., Huang, K., Nakanishi, T., Røsjorde, A., Ohmori, T., Endo, A., Yamamoto, T., 2006. Energy saving in multicomponent separation using an internally heat-integrated distillation column (HIDiC). Applied Thermal Engineering 26 (13), 1362–1368.

Kaibel, G., Blass, E., Koehler, J., 1989. Gestaltung destillativer Trennungen unter Einbeziehung thermodynamischer Gesichtspunkte. Chemie-Ingenieur-Technik 61, 16–25.

Kayihan, F., 1980. Optimum distribution of heat load in distillation columns using intermediate condensers and reboilers. In: Recent Advances in Separation Techniques II. AIChE Symposium Series 192, vol. 76, pp. 1–5.

Kister, H., 1992. Distillation Design. McGraw-Hill, New York.

Koehler, J., Aguirre, P., Blass, E., 1991. Minimum reflux calculations for non-ideal mixtures using the reversible distillation model. Chemical Engineering Science 46, 3007–3021.

Manley, D.B., Chan, P.S., Crawford, D.B., 1992. Thermodynamic analysis of ethylene plant distillation columns. In: AIChE Spring National Meeting.

Naka, Y., Terashita, M., Hayashiguchi, S., Takamatsu, T., 1980. An intermediate heating and cooling method for a distillation column. Journal Chemical Engineering Japan 13, 123–129.

Nakaiwa, M., Huang, K., Endo, A., Ohmori, T., Akiya, T., Takamatsu, T., 2003. Internally heat-integrated distillation columns: a review. Chemical Engineering Research and Design 81 (1), 162–177.

Petlyuk, F., Danilov, R., Serafimov, L., 2008. Trees of reversible distillation trajectories and the structure of trajectory bundles for sections of adiabatic columns. Theoretical Foundations of Chemical Engineering 42 (6), 795–804.

Rivero, R., 2001. Exergy simulation and optimization of adiabatic and diabatic binary distillation. Energy 26 (6), 561–593.

Røsjorde, A., Kjelstrup, S., 2005. The second law optimal state of a diabatic binary tray distillation column. Chemical Engineering Science 60 (5), 1199–1210.

Seader, J., Henley, E., 2006. Separation Process Principles, 2nd ed. Wiley, New York.

Smith, R., 2005. Chemical Process Design and Integration. Wiley, New York.

Soares Pinto, F., 1999. Thermodynamic Analysis of Distillation. Ph.D. Thesis, UMIST, UK.

Stichlmair, J., Herguijuela, J.R., 1992. Separation regions and processes of zeotropic and azeotropic ternary distillation. AIChE Journal 38 (10), 1523–1535.

Terranova, B.E., Westerberg, A.W., 1989. Temperature–heat diagrams for complex columns. 1. Intercooled/interheated distillation columns. Industrial and Engineering Chemistry Research 28, 1374–1379.

Wang, J.C., Henke, G.E., 1966. Tridiagonal matrix for distillation. Hydrocarbon Proceedings 45 (8), 155–163.

Zemp, R.J. 1994. Thermodynamic Analysis of Separation Processes. Ph.D. Thesis, UMIST, UK.